Horseshoe implications

Gabriel B. Mindlin and Ricardo López-Ruiz
Departamento de Fisica y Matemática Aplicada, Facultad de Ciencias, Universidad de Navarra, E-31080, Pamplona (Navarra), Spain

Hernán G. Solari
Departamento de Fisica, FCEN-Universita de Buenos Aires, Pabillon I, Ciudad Universitaria, 1428 Buenos Aires, Argentina

R. Gilmore
Department of Physics & Atmospheric Science, Drexel University, Philadelphia, PA 19104
(Received 16 June 1993)

We have computed all the orbit-forcing implications, up to period 8, in horseshoe-type flows or maps that generate strange attractors. The results are presented in a horseshoe implication diagram. We describe how this diagram was computed, and show how it can be used to construct a minimal (basis) set of periodic orbits which force the existence of all the periodic orbits associated with a strange attractor, up to any given period.

PACS number(s): 05.45.+b

I. INTRODUCTION

Unstable periodic orbits form the backbone of chaotic flows [1–3]. They have recently been used to provide a discrete topological classification of flows for low-dimensional dynamical systems [4]. By low we mean specifically n-dimensional dynamical systems ($n \geq 3$) with a strongly contracting strange attractor having one unstable direction [5]. The Lyapunov exponents for such an attractor satisfy $\lambda_1 > \lambda_2 = 0 > \lambda_3 > \cdots \geq \lambda_n$, where $\lambda_1 < |\lambda_3| \leq \cdots \leq |\lambda_n|$ (strongly contracting condition). By the Kaplan-Yorke conjecture [6], the (Lyapunov) dimension of such an attractor is $d_L = 2 + \lambda_1/|\lambda_3| < 3$.

Topological analyses to identify a template [4,5,7,8] have now been carried out for a number of experimental systems [8–11]. The first step is to locate unstable periodic orbits in the strange attractor. This is conveniently done with experimental data sets by the method of close returns [8]. The next step is to compute the linking numbers [12] for all pairs of surrogate periodic orbits after establishing a three-dimensional embedding. These linking numbers overdetermine a template. The linking numbers of the period-1 and -2 orbits are sufficient to identify the template [4,5,7,8]. The remaining linking numbers are then used either to confirm or invalidate this identification.

In original intent, templates were introduced to describe the organization of all possible periodic orbits of period $p\,(=1,2,3,\ldots)$ built from n symbols, where an orbit of period p has symbolic dynamics $(\sigma_1\sigma_2\cdots\sigma_p)$, with $\sigma_i = 0,1,2,\ldots,n-1$ [Ref. 7]. In the completely hyperbolic, or full shift on n symbol limit, all possible combinations of the σ_i can occur. In analyses of experimental data, we have always found that not all possible periodic orbits, or symbol sequences, are present [8–11]. We have therefore found it fruitful to consider that the flow is restricted to some subportion of a template [5,8] which provides the underlying topological organization for the flow and the periodic orbits in it. As experimental conditions or control parameters are varied, the flow moves over different portions of the template, with new periodic orbits created and old ones annihilated by standard generic bifurcations, which are saddle-node and period doubling bifurcations in horseshoe dynamics.

The orbits which are associated with a flow are not totally independent. The presence of one orbit may require the flow in phase space in its neighborhood to stretch and fold in such a way that other orbits must be present. We then say that the first orbit "forces" the existence of the latter orbits. The conditions under which one orbit forces the existence of another have been discussed in terms of linking numbers [12] and braid theory [13–16].

These phenomena are very clearly seen in the analysis of about 20 data sets for the laser with saturable absorber taken under a variety of experimental conditions [9]. In each case the flow was restricted to a subportion of a Smale horseshoe [17] template. As the experimental conditions varied, the flow was restricted to different portions of the template. Furthermore, under each experimental condition there was a small number of orbits whose existence appeared to force the presence of all the other periodic orbit which were extracted from the data.

In view of these results, the goal of a topological analysis should be twofold: (i) identify a template underlying the strange attractor, and (ii) identify a minimal set of periodic orbits which force all the periodic orbits associated with ("in") the strange attractor. The second objective can be carried out once an orbit implication (or forcing) diagram has been constructed.

We do this in the present work, for systems with horseshoe dynamics, for two reasons. On the theoretical side, templates can arise from either heteroclinic connections or homoclinic connections. Heteroclinic connections can create many different kinds of templates, including a Smale horseshoe [17]. However, homoclinic connections will always generate a Smale horseshoe. On the experimental side, most of the data sets for which to-

pological analyses have been completed have strange attractors generated by a Smale horseshoe [8–11].

The main result of this work is summarized in the horseshoe implication diagram [Fig. 1(a)]. This diagram contains all horseshoe orbits up to period 8. The orbits are identified by their U-sequence labels: the order in which they are created in unimodal maps of the interval. This order is given (to period 11) by Metropolis, Stein, and Stein [18], along with the symbolic dynamics of each orbit [19]. This order is summarized in Fig. 1(b). The symbolic dynamics of these orbits, and some of their other useful properties, have been collected in Table I. In Fig. 1(a) the orbits are located by their U-sequence order along the horizontal axis and their topological entropy along the vertical axis. The presence of one orbit forces the existence of all orbits connected to it by any sequence of links which propagates downward and to the left. For example, 8_8 forces $7_2(8_8 \Longrightarrow 7_2)$ and $7_2 \Longrightarrow 6_1$, so $8_8 \Longrightarrow 6_1$. Conversely, an orbit is forced by any orbit connected to it by a sequence of upward and rightward propagating links (8_2 is forced by 7_2, 8_8, 8_6, 8_5, etc.).

We include orbits only up to period 8 in Fig. 1 for a practical reason. As a general rule, the higher the period, the more difficult it is to extract the orbit from data. In our experience, period 8 is a practical upper bound on the orbits which can be extracted from data and used for topological analyses.

The remainder of this work provides a description of how Fig. 1(a) was constructed and how it can be used. In Sec II we describe how linking numbers provide information about the order in which orbits can be created as a horseshoe is being developed. We also discuss the transitivity of implications, and the care which must be taken when two or more saddle node pairs have the same braid type, and can therefore participate in "exchange elimination." In Sec. III we order the orbits in terms of their topological entropy and U-sequence order. This ordering already provides some information about the structure of

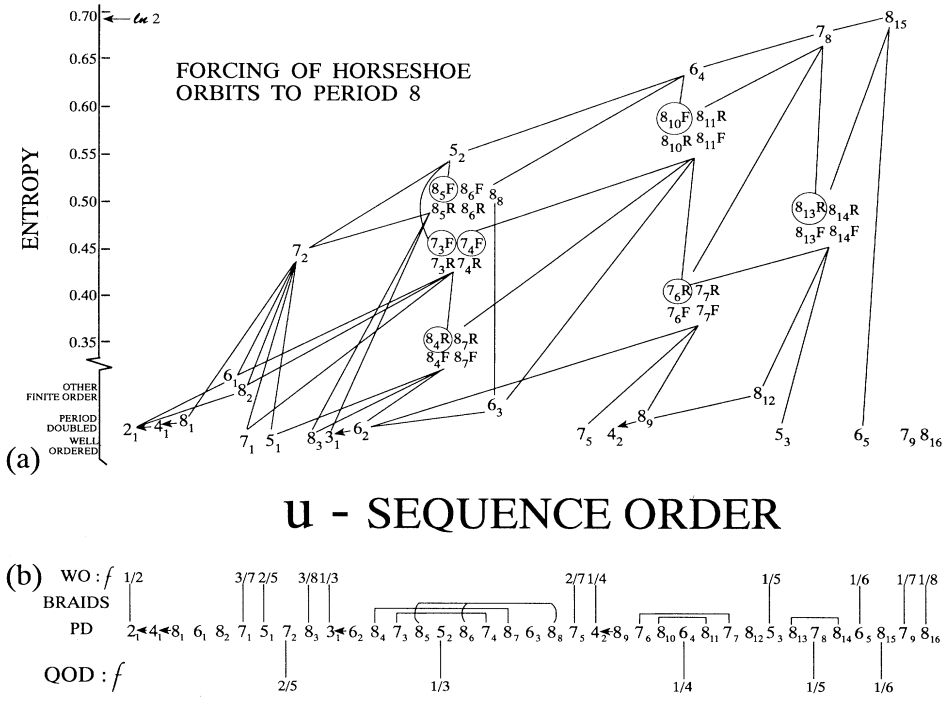

FIG. 1. (a) Horseshoe implication diagram. Orbit B forces A if B is connected to A by a set of links propagating downward and to the left. Orbits are labeled by the order of their creation in the U sequence. Axes are the order of creation in the U sequence (horizontal) and topological entropy (vertical). The zero-entropy orbits are distinguished according to whether they are well ordered, period doubled, or other finite-order orbits. Well ordered orbits form the lower boundary for this diagram and quasi-one-dimensional orbits lie along an arc which forms the upper boundary. When only one member of a braid is forced, this is indicated explicitly as in the case $6_4 \Longrightarrow 8_{10}F$ or $[8_{10}, 8_{11}] \Longrightarrow 7_6R$. When only one member of a braid forces an orbit, this is also indicated explicitly, as in the case $8_8 \Longrightarrow 6_3$. (b) Universal sequence, to period 8. Rational fractional value $f = p/(q+2p)$ is shown for all well-ordered orbits of period $q+2p$ (WO:f). Orbits of the same braid type are tied together. Mother-daughter pairs of period-double orbits are indicated by an arrow. Rational fractional value $f = m/n$ is shown for all quasi-one-dimensional orbits of period $n+2$ (QOD:f). All orbits not WO or QOD lie in an interval bounded by orbits of this type in both parts of this figure. Orbits which are not WO, QOD, PD, and do not belong to a braid multiplet, are other finite-order orbits.

the forcing diagram. We also indicate how portions of the linking number table can be used to infer the structure of the forcing diagram. In Sec. IV we show how to provide a finite description of a strange attractor in terms of a finite basis set of periodic orbits, and how to use the forcing diagram to construct this basis set, which is unique in number and order of orbits up to any given period. We conclude in Sec. V by comparing our topological approach for constructing forcing diagrams with two other recently proposed approaches for determining bifurcation sequences in horseshoe maps.

II. LINKING NUMBERS

During the creation of a horseshoe, periodic orbits are created in a variety of bifurcations, including saddle node and period doubling bifurcations. In multiparameter families of maps and flows, more complex bifurcations can occur [20]. In one parameter families with symmetry (e.g., the Duffing oscillator) additional bifurcations can occur. However, the symmetry forces the underlying template to have more than two branches, and periodic orbits require more than two symbols for their descrip-

TABLE I. Useful properties of the horseshoe orbits to period 8. Orbits are identified as P_U, where P is the period and U is the order of occurrence of the orbit among those of the same period in the U sequence [cf. Fig. 1(b)]. For each orbit, the symbolic sequence is given. If a saddle-node partner exists, it is obtained by changing the parity of the underlined symbol. The permutation of the orbit, either as an orbit in a unimodal map or as an orbit on a Smale horseshoe template, is given. Orbits are identified according to type: WO: well ordered; PD; period doubled; FO: other finite order; PE; positive entropy but not QOD; QOD quasi-one-dimensional. Rational fractional values of WO and QOD orbits are given. The entropy of the orbit in unimodal mappings (one-dimensional entropy) is given, followed by the topological entropy. The two are equal only for QOD orbits.

Orbit	Symbol sequence	Permutation	Remarks	One-dimensional entropy	Topological entropy
2_1	01	12	PD of $1F$	0	0
3_1	0$\underline{1}$1	123	WO $\frac{1}{3}$	0.481 212	0
4_1	0111	1324	PD of 2_1	0	0
4_2	00$\underline{1}$1	1234	WO $\frac{1}{4}$	0.609 378	0
5_1	011 $\underline{1}$1	134 25	WO $\frac{2}{5}$	0.414 013	0
5_2	001 $\underline{1}$1	124 35	QOD $\frac{1}{3}$	0.543 535	0.543 535
5_3	000 $\underline{1}$1	123 45	WO $\frac{1}{5}$	0.656 256	0
6_1	011 1$\underline{1}$1	143 526	FO	0.240 606	0
6_2	001 011	135 246	PD of 3_1	0.481 212	0
6_3	001 1$\underline{1}$1	124 536	FO	0.583 557	0
6_4	000 1$\underline{1}$1	123 546	QOD $\frac{1}{4}$	0.632 974	0.632 974
6_5	000 0$\underline{1}$1	123 456	WO $\frac{1}{6}$	0.675 975	0
7_1	011 11$\underline{1}$1	145 3627	WO $\frac{3}{7}$	0.382 245	0
7_2	011 01$\underline{1}$1	146 2537	QOD $\frac{2}{5}$	0.442 138	0.442 138
7_3	001 01$\underline{1}$1	136 2547	PE	0.522 315	0.476 818
7_4	001 11$\underline{1}$1	125 4637	PE	0.562 400	0.476 818
7_5	001 10$\underline{1}$1	135 6247	WO $\frac{2}{7}$	0.601 001	0
7_6	000 10$\underline{1}$1	124 6357	PE	0.618 362	0.382 245
7_7	000 11$\underline{1}$1	123 5647	PE	0.645 710	0.382 245
7_8	000 01$\underline{1}$1	123 4657	QOD $\frac{1}{5}$	0.666 215	0.666 215
7_9	000 00$\underline{1}$1	123 4567	WO $\frac{1}{7}$	0.684 905	0
8_1	011 101 01	154 726 38	PD of 4_1	0	0
8_2	011 111 $\underline{1}$1	154 637 28	FO	0.304 688	0
8_3	011 011 $\underline{1}$1	147 256 38	WO $\frac{3}{8}$	0.468 258	0
8_4	001 011 $\underline{1}$1	137 256 48	PE	0.499 747	0.346 034
8_5	001 010 $\underline{1}$1	136 472 58	PE	0.539 792	0.498 093
8_6	001 110 $\underline{1}$1	136 572 48	PE	0.547 612	0.498 093
8_7	001 111 $\underline{1}$1	125 647 38	PE	0.574 865	0.346 034
8_8	001 101 $\underline{1}$1	125 736 48	PE	0.591 718	0.498 093
8_9	000 100 11	135 724 68	PD of 4_2	0.609 378	0
8_{10}	000 101 $\underline{1}$1	124 736 58	PE	0.626 443	0.568 666
8_{11}	000 111 $\underline{1}$1	123 657 48	PE	0.639 190	0.568 666
8_{12}	000 110 $\underline{1}$1	124 673 58	FO	0.651 766	0
8_{13}	000 010 $\underline{1}$1	123 574 68	PE	0.660 791	0.458 911
8_{14}	000 011 $\underline{1}$1	123 467 58	PE	0.671 317	0.458 911
8_{15}	000 001 $\underline{1}$1	123 457 68	QOD $\frac{1}{6}$	0.680 477	0.680 477
8_{16}	000 000 $\underline{1}$1	123 456 78	WO $\frac{1}{8}$	0.689 121	0

tion.

For these reasons, we consider in this work only one-parameter families of maps and flows without symmetry leading to the creation of a Smale horseshoe. In such families the only bifurcations which occur generically are saddle node and period doubling bifurcations. Typically, in the development of a horseshoe a pair of periodic orbits is created in a saddle node bifurcation (saddle node pair) [21]. One is a regular saddle. The other is a stable node. In the progression to the fully developed horseshoe, the node loses its stability in a period doubling bifurcation, becoming a "flip saddle" and giving rise to a daughter orbit of twice the period (mother-daughter pair). This daughter orbit, stable at the time of its creation, then loses its stability, undergoing a period doubling bifurcation, etc. In the fully hyperbolic limit the regular (flip) saddle passes an even (odd) number of times through the orientation reversing component (1) of the horseshoe template, so its symbolic description contains an even (odd) number of symbols 1. The orientation of neighborhoods of this orbit are preserved (reversed) when the orbit returns to its initial condition.

In the completely hyperbolic limit all periodic symbol sequences of period p ($\sigma_1\sigma_2\cdots\sigma_p$), $\sigma_i=0,1$, are present, so that the number of orbits of period p is $N(p)\sim 2^p/p\sim(1/p)e^{p\ln(2)}$. The order in which the periodic orbits are created depends on the route taken to the fully hyperbolic limit. This depends in detail on the family of flows or orientation preserving maps considered and the path taken in the space of their control parameters. However, independent of details, some orbits must be created before others are created [13–16]. Conversely, when a horseshoe is "unfolded", some orbits must be destroyed ("pruned") before others [22].

The order in which orbits are forced can be determined from their linking numbers [12]. The linking numbers between all pairs of orbits can be computed in the fully hyperbolic limit, where all periodic orbits exist. These linking numbers remain invariant as long as the orbits exist. Forcing information can be determined from the linking numbers as follows. We consider two pairs of orbits, A and B. We assume no other orbits have the same braid type as A, and similarly for B. We further assume that A and B are saddle node pairs, consisting of a regular and a flip saddle {AR,AF} and {BR,BF}. The linking numbers between these two pairs of orbits can exhibit the possibilities shown in Fig. 2. When all four linking numbers are equal [Fig. 2(b)], neither pair forces the other. However, if the linking numbers between AR and {BR,BF} are equal, but different from the linking numbers between AF and {BR,BF}, then the pair {AR,AF} must be created before the pair {BR,BF} (or B must be annihilated before A can be annihilated), as shown in Fig. 2(a). Under these conditions, if orbits B are present, orbits A must also be present, so that B forces A, or $B\Longrightarrow A$. The third possibility, shown in Fig. 2(c), is that A forces B ($A\Longrightarrow B$).

A similar analysis can be carried out replacing either saddle node pair by a mother-daughter pair. We illustrate with the example of the period-three mother orbit 001 and the period-six daughter orbit 001011. Two iterations of the mother orbit and the daughter orbit (001 001, 001 011) can be treated formally like a saddle node pair of orbits {AR,AF} with the period of the daughter orbit. The linking number calculations in which either (or both) saddle node pairs is replaced by mother daughter pairs proceeds exactly as shown in Fig. 2.

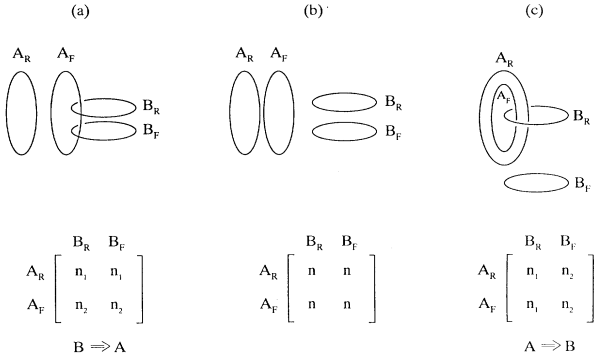

FIG. 2. Linking numbers for two saddle-node pairs. (a) If the linking numbers between AR and {BR,BF} are equal, but different from the linking numbers between AF and {BR,BF}, then the pair AR,AF must be created before the pair BR,BF. (b) When all four linking numbers are equal, neither pair forces the other. (c) If the linking numbers between BR and {AR,AF} are equal, but different from the linking numbers between BF and {AR,AF}, then the pair AR,AF must be created after the pair BR,BF. A similar analysis holds with mother-daughter pairs of period-doubled orbits.

The implications analysis carried out by linking numbers is subject to two additional conditions. These are the possibility of exchange elimination and the transitivity of implications. Both concepts are illustrated in Fig. 3.

Exchange elimination is illustrated in Fig. 3(a). A linking number analysis may indicate that $A\Longrightarrow B$ and $A\Longrightarrow C$. However, if B and C have the same braid type, [13–16,23] then BR and CR can exchange saddle node

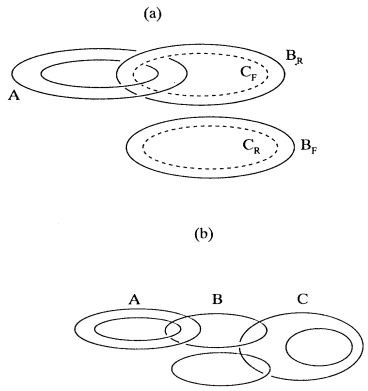

FIG. 3. (a) Exchange elimination: a linking number analysis (Fig. 2) may indicate that $A\Longrightarrow B$ and $A\Longrightarrow C$. If B and C have the same braid type, then {BR,CF} could be formed in one saddle node bifurcation and {BF,CR} in another. Then orbit pair A cannot force any of the four orbits in the quartet {B,C}. (b) The transitivity of forcing: if $A\Longrightarrow B$ and $B\Longrightarrow C$, then $A\Longrightarrow C$.

partners so that {BR,CF} form a saddle node pair while {BF,CR} form another. In the case shown, orbit pair A cannot force any of the four orbits in the quartet {B,C}. This means that the linking numbers must be computed between orbit multiplets of the same braid type rather than just between the saddle node pairings which occur in the U sequence. Period is a braid type invariant, so that only orbits of the same period can be of the same braid type and participate in exchange elimination.

The transitivity of forcing is illustrated in Fig. 3(b). If $A \Longrightarrow B$ and $B \Longrightarrow C$, then $A \Longrightarrow C$. This allows us to reduce the complexity of a forcing diagram. Instead of showing all possible implications, it is sufficient to show only the first order forcings, up to any given period. For example, by direct computation $6_4 \Longrightarrow 8_7$. It is not necessary to show this forcing in Fig. 1, since $6_4 \Longrightarrow 8_{10} \Longrightarrow 8_7$. If A does not force C by direct linking number computation, but $A \Longrightarrow B$ and $B \Longrightarrow C$, then $A \Longrightarrow C$. If there is no intermediate orbit B of low period (≤ 8 in Fig. 1), then the linking number calculations will not reveal that $A \Longrightarrow C$ up to that period.

III. COMPUTATIONAL DETAILS

A. Topological entropy

Strictly speaking, topological entropy is a function of flows or maps, not individual orbits in the flows or maps [13–16]. However, we can define the topological entropy of an orbit as the minimum of the topological entropies of all flows or maps containing an orbit of the same braid type. The topological entropy of an orbit is bounded above by the entropy of that orbit in unimodal maps of the interval. The topological entropy of an orbit A, $\lambda(A)$, provides an estimate of the minimum number of orbits of period p which are forced by A in the set of all flows or maps possessing orbit A: $N(p) \sim (1/p)e^{p\lambda(A)}$.

The topological entropy provides a rough ordering for orbits, since orbits of lower entropy cannot force orbits of higher entropy. Similarly, the U-sequence order for orbits of unimodal maps of the interval provides a rough ordering for horseshoe orbits, since orbits created earlier in the U sequence cannot force orbits created later. Topological entropy and U sequence order provide the two convenient axes on which to present the horseshoe orbit implication diagram.

The one-dimensional entropy for all orbits up to period 8 in unimodal maps of the interval was computed using an algorithm suitable for one-dimensional maps [24]. The topological entropy for these same orbits was also computed [16,25] using recently proposed algorithms [26–28]. The results are summarized in Table I. The one-dimensional entropy increases monotonically with U-sequence order, except for the period-doubled orbits. The entropy of orbits in one dimensional maps provides an upper bound on their topological entropy, which is saturated in certain exceptional cases labeled quasi-one-dimensional (QOD) in Table I.

For convenience, the horseshoe orbits are divided into two groups by their topological entropy, the zero-entropy orbits and the positive-entropy orbits, discussed in the following two sections.

B. Zero-entropy orbits

Zero-entropy or finite-order orbits force only an algebraically growing number of orbits of higher period. All zero-entropy orbits are isotopic to torus knots or iterated torus knots [23]. A simple algorithm exists to identify finite-order orbits. There are two well-known classes of zero-entropy orbits: the well-ordered and the period-doubled orbits.

Well-ordered orbits do not force the existence of any other orbits, except for the period-one orbits $\{1R, 1F\}$, which are forced by all horseshoe orbits and which are therefore not shown in Fig. 1. The symbolic dynamics of a well-ordered orbit of period $q+2p$ consists of q symbols 0 and p symbol sequences 11 "as equally spaced as possible [23]." The irreducible rational fraction $p/(q+2p)$ uniquely identifies each well-ordered orbit. The symbol sequence of the well-ordered orbit with irreducible rational fraction $p/(q+2p)$ is $W(1)W(2)\cdots W(q+p)$, where

$$W(i)=\begin{cases}0 & \text{if } [if]-[(i-1)f]=0\\ 11 & \text{if } [if]-[(i-1)f]=1\end{cases}, \tag{1a}$$

$f=p/(q+p)$, $1 \leq i \leq q+p$, and $[x]$ is the greatest integer in x. For example, the well-ordered orbits of period 7 are determined by the irreducible rational fractions $\frac{3}{7}$ (7_1:011 1111), $\frac{2}{7}$ (7_5;001 1011), and $\frac{1}{7}$ (7_9:000 0011). The saddle node partner of each orbit is obtained by changing the penultimate symbol from 1 to 0. The well-ordered horseshoe orbits to period 8 are $(7_1, 5_1, 8_3, 3_1, 7_5, 4_2, 5_3, 6_5, 7_9, 8_{16})$. They are identified by their fractional values, which decrease in the order of their creation in the U sequence [cf. Fig. 1(b) and Table I]. They are also shown along the horizontal (zero-entropy) axis of Fig. 1(a).

(ii) Period-doubled daughter orbits force only their mother (and grandmother, etc.) orbits. The period-doubled orbits, to period 8, are $[8_1 \Longrightarrow 4_1 \Longrightarrow 2_1,\ 6_2(\Longrightarrow 3_1),\ 8_9(\Longrightarrow 4_2)]$. They are clearly identified in Figs. 1(a) and 1(b).

The remaining finite-order orbits to period 8 are $(6_1, 8_2, 6_3, 8_{12})$. These force only the orbits shown in Fig. 1(a). The self-relative rotation rates of the zero-entropy orbits easily distinguish between the well-ordered and period-doubled orbits. For the well-ordered orbit corresponding to the rational fraction $p/(q+2p)$ all relative rotation rates are $p/(q+2p)$; for period-doubled orbits the systematics of the self-relative rotation rates are given in Ref. [12].

C. Positive-entropy orbits

Positive-entropy orbits force an exponentially growing number of orbits of higher period. The positive-entropy orbits fall in two classes. These are the quasi-one-dimensional orbits (QOD) and the remaining positive entropy orbits.

(i) Quasi-one-dimensional orbits force all the orbits in two-dimensional maps as they force in one-dimensional maps of the interval. In this sense they are dual to the well-ordered orbits, which force only the period one or-

bits $\{1R,1F\}$. Like the well-ordered orbits, there is a 1-1 correspondence between the QOD orbits and the irreducible rational fractions in the interval $(0,\frac{1}{2})$ [14,16]. To each irreducible rational fraction $0<f=m/n<\frac{1}{2}$ there corresponds a QOD orbit of period $n+2$ with symbolic dynamics $0^{\kappa_1(f)}110^{\kappa_2(f)}11\cdots110^{\kappa_m(f)}111$, where

$$\kappa_1(f)=[1/f]-1=[n/m]-1\ ,$$
$$\kappa_i(f)=[i/f]-[(i-1)/f]-2$$
$$=[in/m]-[(i-1)n/m]-2\ ,\quad 2\le i\le m\ . \quad (1b)$$

For example, the QOD orbits of period 7 are determined by the irreducible rational fractions $\frac{2}{5}$ (7_2:011 0111) and $\frac{1}{5}$ (7_8:000 0111). The saddle node partner of each is obtained by changing the penultimate symbol from 1 to 0.

The QOD orbits to period 8 are $(7_2,5_2,6_4,7_8,8_{15})$. Their corresponding rational fractional values are shown in Fig. 1(b) and Table I. Each QOD saddle node pair belongs to a braid type containing no other horseshoe orbits. The entropy of the QOD orbits is the same for three-dimensional flows and two dimensional maps as for one-dimensional maps of the interval.

(iii) The remaining positive-entropy orbits consist of those orbits not previously discussed. For these orbits, two or more saddle pairs always belong to the same braid type. Orbits of the same braid type were identified by their spectrum of relative rotation rates. This topological index is sufficient to identify braid type through orbits of period 10 [29]. Orbits of the same braid type have the same entropy.

The positive-energy orbits were organized in order of increasing topological entropy; those with the same topological entropy were organized by order of occurrence in the universal sequence, or one-dimensional entropy. This order is $\{[8_4,8_7],[7_6,7_7],\ 7_2,\ [8_{13},8_{14}],[7_3,7_4],[8_5,8_6;8_8],\ 5_2,[8_{10},8_{11}],6_4,7_8,8_{15}\}$. In this ordering no earlier orbit can force a later orbit. Orbits within square brackets [ ] have the same braid type, and can therefore participate in exchange elimination. In the sextet, the linking number calculations show that 8_5 and 8_6 are more similar to each other than to 8_8: in particular, 8_5 and 8_6 participate in exchange elimination but 8_8 does not. In addition, 8_8 forces 6_3 as well as the orbits forced by 8_5 and 8_6. Orbits with unique braid type (e.g., 7_2) are QOD.

The linking numbers of all 18 pairs of positive entropy orbits were computed. We do not reproduce the entire linking number table here. Rather, we reproduce some submatrices of this table in Fig. 4.

In Fig. 4(a) we reproduce the linking numbers between the quartets $[8_4,8_7]$ and $[7_3,7_4]$. These results show that $7_3\Longrightarrow 8_4\ R$, $7_4\Longrightarrow 8_4\ R$. In fact, any orbit in the quartet $[7_3,7_4]$ forces $8_4\ R$, which may be paired with either $8_4\ F$ or $8_7\ F$.

In Fig. 4(b) we reproduce the linking numbers between the lower entropy quartet $[7_6,7_7]$ and the higher entropy sextet $[8_5,8_6,8_8]$. This appears to show that $7_6\Longrightarrow 8_5, 7_6\Longrightarrow 8_6$, and similarly for 7_7 [cf. Fig. 3(a)]. However, once both 8_5 and 8_6 exist, 8_5R and 8_6R can exchange flip saddles, so that in fact $[7_6,7_7]$ do not force $[8_5,8_6]$ by exchange elimination [cf. Fig. 3(b)].

In Fig. 4(c) we show the linking numbers between the quartet $[8_4,8_7]$ and the quartet $[8_{10},8_{11}]$. This clearly shows $[8_{10},8_{11}]\Longrightarrow[8_4,8_7]$.

D. Zero and positive-entropy orbits

The linking numbers between the zero-entropy orbits and the positive-entropy orbits were then computed to complete the forcing diagram. The interpretation of the linking number table was straightforward. We make a few remarks about the construction of Fig. 1(a).

(i) It is possible to locate each periodic orbit by its one-dimensional entropy, or entropy in unimodal maps (horizontal coordinate) and topological entropy, or minimal entropy in two-dimensional maps (vertical coordinate).

(a)

		7_3		7_4	
		F	R	R	F
8_4	R	18	18	18	18
	F	19	19	19	19
8_7	F	19	19	19	19
	R	19	19	19	19

(b)

		8_5		8_6		8_8	
		F	R	R	F	R	F
7_6	R	14	15	14	15	15	15
	F	14	15	14	15	15	15
7_7	F	14	15	14	15	15	15
	R	14	15	14	15	15	15

(c)

		8_{10}		8_{11}	
		F	R	R	F
8_4	R	18	18	18	18
	F	19	19	19	19
8_7	F	19	19	19	19
	R	20	20	20	20

(d)

		8_5		8_6		8_8	
		F	R	R	F	R	F
6_3	R	14	15	14	15	14	14
	F	14	15	14	15	15	15

FIG. 4. Four sections of the linking number table for horseshoe orbits up to period 8. (a) Linking numbers between the quartets $[8_4,8_7]$ and $[7_3,7_4]$. Any of the quartet of orbits $[7_3,7_4]$ forces 8_4R which may be paired with either 8_4F or 8_7F. (b) Linking numbers between the lower-entropy quartet $[7_6,7_7]$ and the higher-entropy sextet $[8_5,8_6,8_8]$. Once both 8_5 and 8_6 exist, 8_5R and 8_6R can exchange flip saddles, so that $[7_6,7_7]$ do not force $[8_5,8_6]$, by exchange elimination. (c) Linking numbers between the quartet $[8_4,8_7]$ and $[8_{10},8_{11}]$ show $[8_{10},8_{11}]\Longrightarrow[8_4,8_7]$. (d) Linking numbers for the zero-entropy finite-order orbit 6_3 and the sextet $[8_5,8_6;8_{12}]$ show that the zero-entropy orbit 6_3 can force either 8_5 or 8_6 when just one of the two pairs is present, cannot force either saddle-node pair $8_5R,8_6F$ or $8_5F,8_6R$, and cannot force either 8_5 or 8_6 when both are present, by exchange elimination.

In such a representation all zero-entropy orbits lie on the horizontal axis and all QOD orbits, for which the topological entropy saturates the one-dimensional entropy, lie on the equal entropy diagonal. All remaining orbits lie between these two limits. Orbits of the same braid type are easily identified as having the same vertical coordinate. In practice, this representation suffers from two difficulties. First, period-doubled orbits in a cascade are degenerate. Second, such a diagram is difficult to read because of the compression due to increasing density of orbits with increasing entropy. In constructing Fig. 1(a) we have adjusted the positions of orbits somewhat to make the figure more legible. The zero-entropy orbits have been placed on three levels depending on whether they are well ordered, period doubled, or other finite order. The lower and upper boundaries for this diagram then consist of well-ordered and quasi-one-dimensional orbits. We further observe that every other orbit belongs to an interval in the U sequence which is bounded on the left and right by either a well-ordered or a QOD orbit. For example, 7_4 is in an interval bounded on the left by 5_2 and on the right by 7_5 in Fig. 1(b). The horizontal locations of all orbits in Fig. 1(a) have been adjusted somewhat within these intervals, but no orbit has been relocated outside its interval.

(ii) Each positive-entropy orbit forces a contiguous sequence of well-ordered orbits. That is, if a positive-entropy orbit forces well-ordered orbits corresponding to the rotational fractions P/Q and P'/Q', it forces all well-ordered orbits with intermediate rational fractional values.

(iii) The linking numbers for the zero-entropy finite-order orbit 6_3 and the sextet $[8_5,8_6;8_8]$ are shown in Fig. 4(d). This is comparable to Fig. 4(b) and shows that the zero-entropy orbit 6_3 can force either 8_5 or 8_6 when just one of the two pairs is present, cannot force either saddle-node pair $\{8_5R,8_5F\}$ or $\{8_5F,8_6R\}$, and cannot force either 8_5 or 8_6 when both are present, by exchange elimination. While 8_8 forces 6_3, neither 8_5 nor 8_6 does.

IV. BASIS SETS OF ORBITS

Our long-range goal is to find a discrete classification for chaotic dynamical systems. A comparable goal is to be able to compare two strange attractors and determine if they are topologically equivalent, that is, if one is a reparametrization of the other. For low-dimensional ($d_L<3$) dynamical systems this goal appears within reach.

The first step is to identify the topology of the embedding space: the manifold containing the strange attractor. In the experimental data sets analyzed so far [8–11], the embedding space has been $D^2\times S^1$ (D^2 is a two-dimensional disk, $D^2\times S^1$ is a solid torus). Identifying the topology of the embedding space is a classical discrete problem.

The next step is to identify a template, or "knot-holder," in the embedding space [3,4,7,8]. This structure is a branched manifold obtained by projecting the flow along the stable direction. The template supports the strange attractor and describes the organization of all the periodic orbits in it. Templates are identified by a set of integer invariants [4]. We have shown how to extract these integers from time series data [8], and this program has now been carried out on a number of experimental data sets [8–11].

The third step is to enumerate all the periodic orbits associated with the strange attractor. This is a very ambitious step, particularly in view of the problem that, both experimentally and mathematically, less information is available about higher period than lower period orbits. Accordingly, we define two strange attractors as topologically equivalent (conjugate, isotopic) to period p if they possess the same spectrum of periodic orbits up to period p. Identifying equivalence classes of strange attractors to some finite period p is analogous to identifying equivalence classes of mappings by their k jets (Taylor series expansions), for some finite k [31].

The problem of determining equivalence to period p is resolved by the appropriate choice of a basis set of periodic orbits, to period p. A basis set is a minimal set of periodic orbits which force all the periodic orbits which are present in a strange attractor, up to some fixed period. This can be done for horseshoe-type strange attractors using Fig. 1(a). We illustrate this idea with an example. If the orbit 7_6 is present in a data set, then to period 8 the five orbits $\{6_2\Longrightarrow 3_1,7_5,8_9\Longrightarrow 4_2\}$ are forced. However, if the flow is highly dissipative, many more orbits will be present. All orbits which occur before 7_6 in the U sequence will be present [Fig. 1(b)] [18]. The basis set for this collection of orbits, to period 8, is uniquely $\{5_2,8_8,8_6F,7_4F,7_6,8_7R\}$. This basis set is easily constructed as follows. All orbits present (i.e., forced by 7_6 in one-dimensional maps) are listed in increasing topological entropy and U-sequence order, as described in Sec. III C. This order is $\{\underline{2}_1,\underline{4}_1,\underline{8}_1,\underline{6}_1,\underline{8}_2,\underline{7}_1,\underline{5}_1,\underline{8}_3,\underline{3}_1,\underline{6}_2,6_3,7_5,4_2,8_9,\underline{8}_4,8_7,7_6,\underline{7}_2,\underline{7}_3,7_4,\underline{8}_5,8_6,8_8,\underline{5}_2\}$. The last orbit in this list is identified as a basis orbit, and all orbits which this orbit forces (they are underlined) are removed from the list. The shortened list is $\{\underline{6}_3,7_5,4_2,8_9,8_7R,7_6,7_4F,8_5,8_6F,8_8\}$. This procedure is repeated on the shortened list. To any period, this is a finite, fast, and efficient algorithm that provides a list of basis orbits unique in both number and order. This algorithm involves orbit removal from top to bottom (decreasing topological entropy), right to left (decreasing one dimensional entropy) in Fig. 1(a).

This procedure is the dynamical system analog of the determination of dimension and choice of basis vectors for a linear system. The choice of a basis set of orbits identifies the subportion of a horseshoe template to which a flow with a given spectrum of periodic orbits is restricted. A lower bound on the entropy of such a flow can be estimated by computing the topological entropy of the (reducible) braid consisting of the basis orbits.

V. SUMMARY AND CONCLUSION

The construction of an orbit forcing diagram, carried out here by topological methods, is intermediate in spirit between two recently proposed approaches to this problem. Hall [14,15] and Tufillaro [16] consider two-dimensional diffeomorphisms and ask the question: which

braids must be present when others are present? They provide machinery for answering this question in general, and Tulfillaro gives explicit answers in the case of orbits forced by the quasi-one-dimensional orbits AB, A^2B, and A^3B of period 7, 10, and 13, with A=011 and B=0111 or 0101.

Cvitanovic, Gunaratne, and Procaccia [22] consider families of dissipative orientation preserving maps and ask the question: which orbits must be missing when others are missing? Their answer is given in terms of a "pruning front" moving through the space of periodic orbits, systematically removing orbits from the hyperbolic limit. This description becomes an increasingly good approximation to the bifurcation sequence as the dissipation of the maps increases.

As in Ref. [22], our topological approach starts from the hyperbolic limit for flows in which all possible horseshoe orbits exist. In this limit the linking numbers of all orbits, up to some particular period, are computed. As in Refs. [14–16], we ask which orbits must exist when others are present. From this information we can infer which orbits must be annihilated before any particular orbit is annihilated ("horseshoe unfolding"). Proceeding in the reverse direction of horseshoe formation, we can infer which orbits must be created before others are formed. This provides a partial order on orbit formation for three dimensional flows and two dimensional orientation preserving maps which evolve into horseshoes under parameter variation. The results are not perturbative, are valid independent of dissipation from the conservative limit (zero dissipation) to the unimodal limit (infinite dissipation), and are given explicitly in Fig. 1(a) up to period 8.

Two flows with isotopic embedding manifolds and identical knot holders are equivalent to period p if they have the same basis set of periodic orbits to period p. The forcing diagram can be used to construct a finite basis set of periodic orbits for any dynamical system which exhibits dynamics compatible with the formation of a Smale horseshoe. We have shown how to construct a basis set for any spectrum of horseshoe orbits, up to any period.

ACKNOWLEDGMENTS

R. G. thanks Nick Tufillaro and Toby Hall for extensive discussions, and we thank both for making their work available to us prior to publication. G. B. M. and R. L-R. received financial support under Grant No. DGICYT (Spanish government) PB90-0632. R.L-R. thanks the Gobierno de Navarra (Spain) for a grant.

[1] R. Devaney and Z. Nitecki, Commun. Math. Phys. **67**, 137 (1979).
[2] D. Auerbach, P. Cvitanovic, J.-P. Eckmann, G. Gunaratne, and I. Procaccia, Phys. Rev. Lett. **58**, 2387 (1987).
[3] P. Cvitanovic, Physica D **51**, 138 (1991).
[4] G. B. Mindlin, X.-J. Hou, H. G. Solari, R. Gilmore, and N. B. Tufillaro, Phys. Rev. Lett. **64**, 2350 (1990).
[5] G. B. Mindlin and R. Gilmore, Physica D **58**, 147 (1992).
[6] J. L. Kaplan and J. A. Yorke, in *Functional Difference Equations and the Approximation of Fixed Points,* edited by H. O. Peitgen and H. O. Walther, Springer Lecture Notes in Mathematics Vol. 730 (Springer-Verlag, Berlin, 1979), p. 204.
[7] J. S. Birman and R. F. Williams, Topology **22**, 47 (1983).
[8] G. B. Mindlin, H. Solari, M. Natiello, X.-J. Hou, and R. Gilmore, J. Nonlinear Sci. **1**, 147 (1991).
[9] F. Papoff, E. Arimondo, F. Fioretto, G. B. Mindlin, H. G. Solari, and R. Gilmore, Phys. Rev. Lett. **68**, 1128 (1992).
[10] N. B. Tufillaro, R. Holzner, L. Flepp, E. Brun, M. Finardi, and R. Badii, Phys. Rev. A **44**, 4786 (1991).
[11] P. Glorieux and M. LeFranc, Int. J. Bifurcation Chaos (to be published).
[12] H. G. Solari and R. Gilmore, Phys. Rev. A **37**, 3096 (1988).
[13] P. Boyland, Comtemp. Math. **81**, 119 (1988).
[14] T. D. H. Hall, Ph.D. thesis, University of Cambridge, 1991 (unpublished).
[15] T. Hall, Phys. Rev. Lett. **71**, 58 (1993).
[16] N. B. Tulfillaro, (unpublished).
[17] S. Smale, Bull. Am. Math. Soc. **73**, 747 (1967).
[18] N. Metropolis, M. L. Stein, and P. R. Stein, J. Combinatorial Theory **15**, 25 (1973).
[19] J. Milnor and W. Thurston, in *Dynamical Systems,* edited by J. Alexander, Springer Lecture Notes in Mathematics Vol. **1342** (Springer-Verlag, Berlin, 1988), p. 465.
[20] R. Gilmore, *Catastrophe Theory for Scientists and Engineers* (Wiley, New York, 1984).
[21] E. Eschenazi, H. G. Solari, and R. Gilmore, Phys. Rev. A **39**, 2609 (1989).
[22] P. Cvitanovic, G. Gunaratne, and I. Procaccia, Phys. Rev. A **38**, 1503 (1988).
[23] P. Holmes and D. Whitley, Philos. Trans. R. Soc. London Ser. A **311**, 43 (1984).
[24] L. Block, J. Guckenheimer, M. Misiurewics, and L.-S. Young, in *Global Theory of Dynamical Systems,* edited by Z. Nitecki and C. Robinson, Springer Lecture Notes in Mathematics Vol. 819 (Springer-Verlag, New York, 1980), p. 18.
[25] T. Hall (unpublished).
[26] M. Bestvina and M. Handel, Ann. Math. **135**, 1 (1992).
[27] J. Los, Proc. London Math. Soc. **66**, 1 (1993).
[28] T. White (unpublished). A copy of this program is available by contacting T. White at the following electronic address: tadpole@ucrmath.ucr.edu.
[29] T. Hall (private communication).
[30] Computer codes for computing the linking numbers and relative rotation rates for periodic orbits are available on request from any of the authors.
[31] M. Golubitsky and V. Guillemin, *Stable Mappings and Their Singularities* (Springer-Verlag, Berlin, 1973).